



저작자표시-비영리-변경금지 2.0 대한민국

이용자는 아래의 조건을 따르는 경우에 한하여 자유롭게

- 이 저작물을 복제, 배포, 전송, 전시, 공연 및 방송할 수 있습니다.

다음과 같은 조건을 따라야 합니다:



저작자표시. 귀하는 원저작자를 표시하여야 합니다.



비영리. 귀하는 이 저작물을 영리 목적으로 이용할 수 없습니다.



변경금지. 귀하는 이 저작물을 개작, 변형 또는 가공할 수 없습니다.

- 귀하는, 이 저작물의 재이용이나 배포의 경우, 이 저작물에 적용된 이용허락조건을 명확하게 나타내어야 합니다.
- 저작권자로부터 별도의 허가를 받으면 이러한 조건들은 적용되지 않습니다.

저작권법에 따른 이용자의 권리는 위의 내용에 의하여 영향을 받지 않습니다.

이것은 [이용허락규약\(Legal Code\)](#)을 이해하기 쉽게 요약한 것입니다.

[Disclaimer](#)

Effect of hepatic steatosis on native T1
mapping of 3T magnetic resonance
imaging in the assessment of T1 values
for patients with non-alcoholic fatty
liver disease

Jhii-Hyun Ahn

Department of Medicine

The Graduate School, Yonsei University

Effect of hepatic steatosis on native T1
mapping of 3T magnetic resonance
imaging in the assessment of T1 values
for patients with non-alcoholic fatty
liver disease

Jhii-Hyun Ahn

Department of Medicine

The Graduate School, Yonsei University

Effect of hepatic steatosis on native T1
mapping of 3T magnetic resonance
imaging in the assessment of T1 values
for patients with non-alcoholic fatty
liver disease

Directed by Professor Jeong-Sik Yu

The Doctoral Dissertation
submitted to the Department of Medicine,
the Graduate School of Yonsei University
in partial fulfillment of the requirements for the degree
of Doctor of Philosophy

Jhii-Hyun Ahn

June 2021

This certifies that the Master's Thesis
(Doctoral Dissertation) of Jhii-Hyun
Ahn is approved.

Thesis Supervisor : Jeong-Sik Yu

Thesis Committee Member#1 :Jae-Joon Chung

Thesis Committee Member#2 : Dal Mo Yang

Thesis Committee Member#3: Ik Jae Lee

Thesis Committee Member#4: Jung Il Lee

The Graduate School
Yonsei University

June 2021

ACKNOWLEDGEMENTS

Until the completion of this Doctor's thesis, professor Jeong-Sik Yu, supervisor, advised and supported me enthusiastically. I am very grateful for this instructions and feedback which kept me focused in my study.

I'm also appreciate professor Jae-Joon Chung's great supporting for my research and advice for me learning science. The precious comments and crucial times given by my commentators, professor Dal Mo Yang, Ik Jae Lee and Jung Il Lee have made the clarification and improvement of this thesis.

I'd like to thank to professor Kyu-Sang Park and Moon Young Kim in Wonju Christian Hospital for practical helps.

I thank to the endless love and care of Bong-Hyuk Ahn and Jung-Sook Lee, my parents. Most of all, I appreciate my husband, Seung Phil Hong, who is deeply in love with me and has always supported me in deep and profound ways. Lastly, I thank my adorable daughter, Soo Min Hong, who has always supported me and made me know deep love.

<TABLE OF CONTENTS>

ABSTRACT	1
I. INTRODUCTION	3
II. MATERIALS AND METHODS	5
1. Subjects	5
2. Clinical data	6
3. MRI protocol	7
(A) MRI-PDFF	7
(B) T1 mapping	8
(C) MRE	9
4. Imaging analysis	9
5. Statistical analysis	10
III. RESULTS	13
1. Subjects	13
2. Correlation between fat fraction from MRI-PDFF and liver stiffness of MRE and T1 value	13
3. T1 value according to hepatic steatosis and liver stiffness	13
4. Univariate and multiple linear regression analyses for variables affecting the T1 value and liver stiffness of MRE	16
5. Reproducibility and repeatability of the MR elastography and T1 mapping	16
IV. DISCUSSION	21
V. CONCLUSION	25
REFERENCES	26
ABSTRACT(IN KOREAN)	33
PUBLICATION LIST	35

LIST OF FIGURES

Figure 1. Flow chart representing subject recruitment	6
Figure 2. Multi-echo Dixon sequences and fat fraction map	8
Figure 3. Representative measurement of liver stiffness and T1 relaxation time using magnetic resonance elastography and T1 mapping	11
Figure 4. Pearson's correlation coefficient	15
Figure 5. Box and whisker plot of the T1 relaxation time according to the hepatic steatosis grade.	17

LIST OF TABLES

Table 1. Equations of non-invasive prediction scored for hepatic steatosis	7
Table 2. Demographic and laboratory characteristics of study subjects	14
Table 3. T1 relaxation time of study subjects classified according to hepatic steatosis	15
Table 4. Results of univariate and multiple linear regression analysis of T1 value	18
Table 5. Results of univariate and multiple linear regression analysis of liver stiffness at MRE	19
Table 6. Reproducibility and repeatability of measurements obtained by MRE and T1 mapping	20

ABSTRACT

Effect of hepatic steatosis on native T1 mapping of 3T magnetic resonance imaging in the assessment of T1 values for patients with non-alcoholic fatty liver disease

Jhii-Hyun Ahn

*Department of Medicine
The Graduate School, Yonsei University*

(Directed by Professor Jeong-Sik Yu)

Objectives: This study investigated whether T1 values in native T1 mapping of 3T magnetic resonance imaging (MRI) of the liver were affected by the fatty component.

Materials and Methods: This prospective study involved 340 participants from a population-based cohort study between May 8, 2018 and August 8, 2019. Data obtained included: (1) hepatic stiffness according to magnetic resonance elastography (MRE); (2) T1 value according to T1 mapping; (3) fat fraction and iron concentration from multi-echo Dixon; and (4) clinical indices of hepatic steatosis including body mass index, waist circumference, history of diabetes, aspartate aminotransferase, alanine aminotransferase, gamma-glutamyl transpeptidase, and triglycerides. The correlations between T1 value and fat fraction, and between T1 value and liver stiffness were assessed using Pearson's correlation coefficient. The independent two-sample *t*-test was used to evaluate the differences in T1 values according to the presence or absence of hepatic steatosis, and the one-way analysis of variance was used to evaluate the difference in T1 value by grading of hepatic steatosis according to MRI-based proton density fat fraction (PDFF). In addition, univariate and multivariate linear regression analyses were performed to determine whether other variables influenced the T1 value.

Results: T1 value showed a positive correlation with the fat fraction obtained from PDFF ($r=0.615$, $P < 0.001$) and with the liver stiffness obtained from MRE ($r=0.370$, $P < 0.001$). Regardless of the evaluation method, the T1 value was significantly increased in subjects with hepatic steatosis ($P < 0.001$). When comparing hepatic steatosis grades based on MRI-PDFF, the mean T1 values were significantly different in all grades, and the T1 value tended to increase as the grade increased ($P < 0.001$, P for trend < 0.001). On multiple linear regression analysis, the T1 value was influenced by MRI-PDFF, calculated liver iron concentration, liver stiffness, and serum aspartate aminotransferase level.

Conclusion: The T1 value obtained by current T1 mapping of 3T MRI was affected by the liver fat component and several other factors such as liver stiffness, iron concentration, and inflammation.

Keywords: T1 mapping, T1 value, hepatic steatosis, nonalcoholic fatty liver disease, liver stiffness, hepatic fibrosis

Effect of hepatic steatosis on native T1 mapping of 3T magnetic resonance imaging in the assessment of T1 values for patients with non-alcoholic fatty liver disease

Jhii-Hyun Ahn

*Department of Medicine
The Graduate School, Yonsei University*

(Directed by Professor Jeong-Sik Yu)

I. INTRODUCTION

Nonalcoholic fatty liver disease (NAFLD) is a leading cause of chronic liver disease (CLD) worldwide, and the worldwide prevalence of NAFLD is estimated to be 25%.^{1,2} NAFLD ranges from simple benign hepatic steatosis to severe hepatocellular inflammation known as nonalcoholic steatohepatitis (NASH).³ Simple benign hepatic steatosis is less likely to develop to progressive liver disease and cirrhosis, but exposure of fatty hepatocytes to insults or stress, causing cell death, apoptosis, inflammation, and fibrosis can lead to NASH.⁴ If hepatic fibrosis develops as NASH progresses, the liver becomes stiff and functionally impaired, which can lead to cirrhosis, hepatocellular carcinoma, death, and/or the need for liver transplantation.⁵

A liver biopsy is the current reference standard for assessing NAFLD. However, a liver biopsy is invasive, there may be sampling errors, and complications such as bleeding or death may occur.^{6,7} Therefore, non-invasive methods, such as imaging techniques and serologic markers, have been developed to diagnose NAFLD, and most of the methods are focused on hepatic fibrosis.⁸

Elastography is a representative imaging technique used to diagnose hepatic fibrosis. Among elastography techniques, magnetic resonance elastography (MRE) is a magnetic resonance imaging (MRI)-based method for quantitatively imaging tissue stiffness. Studies have shown that MRE-based hepatic stiffness measurements represent an accurate method to fibrosis, including early fibrosis.⁹⁻¹¹ However, MRE is limited in obese patients and subjects with ascites.¹² It also requires specialized hardware and software.¹³ Owing to the disadvantages of MRE, there is a need for a technique that can be easily applied.

Studies have shown that T1 value, which is a tissue-specific parameter, correlates with hepatic fibrosis, and T1 value of the liver parenchyma could differentiate healthy subjects from patients with liver cirrhosis.¹⁴⁻¹⁷ T1 mapping can be easily performed without additional hardware and is not affected by obesity or ascites. However, T1 may be affected by histologic factors such as fat, iron, inflammation, and fibrosis.¹⁸ Therefore, in order to use T1 value in the evaluation of patients with NAFLD, the influence of these factors must be investigated. To date, studies using T1 mapping have identified the effects of iron, fibrosis, and inflammation in the liver, but different results have been reported for the effects of liver fat content. Some studies have shown that fat in tissues affects T1 or that liver fat content does not affect T1, whereas other studies have not considered hepatic steatosis.^{16,17,19,20} Liver fibrosis, inflammation, and steatosis are features of NAFLD; therefore, it is necessary to study the effects of hepatic steatosis when assessing NAFLD using T1 mapping.

We assessed whether T1 value was affected by the presence or absence of hepatic steatosis.

II. MATERIALS AND METHODS

1. Subjects

The study subjects were recruited from 1,894 individuals who completed the 3rd follow-up survey (from May 2011 to October 2017) among those already enrolled in a population-based cohort study, the Korean Genome and Epidemiology Study on Atherosclerosis Risk of Rural Areas in the Korean General Population (KoGES-ARIRANG). KoGES-ARIRANG is a population-based cohort study to assess the prevalence, incidence, and risk factors for chronic degenerative disorders such as hypertension, diabetes, metabolic syndrome, and cardiovascular disease.^{21,22} Subjects aged 75 years or older were excluded to enable the conduct of tests, including MRI. In addition, subjects with a clinical history of malignancy, alcohol abuse (men, >30 g/day; women, >20 g/day), and liver disease other than fatty liver, such as viral hepatitis, Wilson disease, hemochromatosis, autoimmune hepatitis, and drug-induced liver injury, were excluded. Further, subjects who did not want to participate in the study were excluded. Subsequently, 348 subjects were enrolled on a consecutive basis between May 8, 2018 and August 8, 2019. Among the 348 enrolled individuals, 8 subjects with incomplete data (MRI failure, n=2; blood sampling failure, n=4; body mass index [BMI] missing, n=2) were additionally excluded, and 340 subjects (122 males and 218 females; mean age, 66.27 ± 7.28 years) were finally included in this analysis (Fig. 1). This prospective study was approved by the institutional review board, and all study subjects provided written informed consent before the investigation.

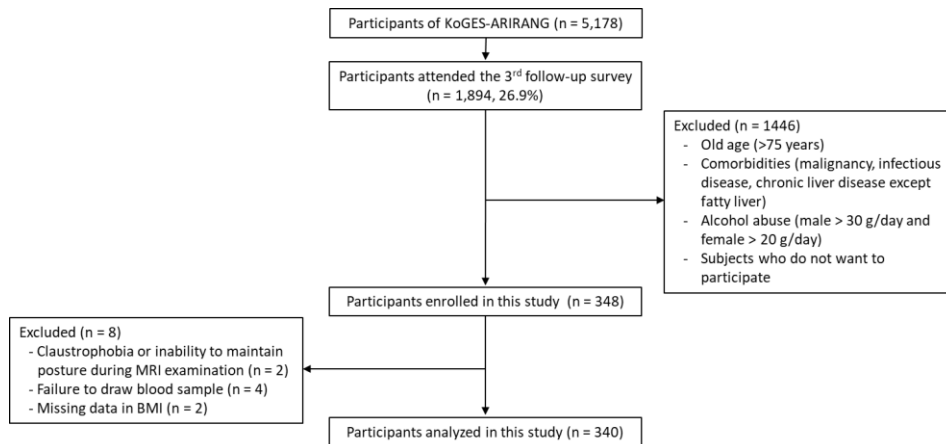


Figure 1. Flow chart representing subject recruitment.

KoGES-ARIRANG, Korean Genome and Epidemiology Study on the Atherosclerosis Risk of Rural Areas in the Korean General Population; MRI, magnetic resonance imaging; BMI, body mass index

2. Clinical data

For all subjects, the following parameters were recorded at the time of the MRI. Clinical parameters included age, gender, BMI, waist circumference, and history of diabetes. Laboratory data included aspartate aminotransferase (AST), alanine aminotransferase (ALT), gamma-glutamyl transpeptidase (GGT), alkaline phosphatase, albumin, complete blood count, total cholesterol level, triglyceride level, high-density lipoprotein cholesterol level, and fasting glucose levels. Diabetes mellitus (DM) was defined as fasting glucose level of 126 mg/dL (7 mmol/L) or greater or treatment with antidiabetic drugs. Using these data, the fatty liver index (FLI),²³ NAFLD liver fat score (NAFLD-LFS)²⁴ and hepatic steatosis index (HSI)²⁵ were calculated. The respective equations are shown in Table 1. The criteria for judging hepatic steatosis in each of the indices

were more than 60 for FLI, greater than -0.640 for NLFS, and greater than 36 for HIS.²³⁻²⁵

Table 1. Equations of non-invasive prediction scored for hepatic steatosis.

Indices	Equation
FLI	$\frac{(e^{0.953 \cdot \text{Loge}(\text{TG}) + 0.139 \cdot \text{BMI} + 0.718 \cdot \text{Loge}(\gamma\text{-GT}) + 0.053 \cdot \text{WC} - 15.745})}{(1 + e^{0.953 \cdot \text{Loge}(\text{TG}) + 0.139 \cdot \text{BMI} + 0.718 \cdot \text{Loge}(\gamma\text{-GT}) + 0.053 \cdot \text{WC} - 15.745})} * 100$
NAFLD-LFS	$-2.89 + 1.18 \cdot \text{Metabolic syndrome (yes = 1, no = 0)} + 0.45 \cdot \text{Diabetes mellitus (yes = 2, no = 0)} + 0.15 \cdot \text{Insulin} + 0.04 \cdot \text{AST} - 0.94 \cdot \text{AST/ALT ratio}$
HIS	$\frac{(e^{0.315 \cdot \text{BMI} + 2.421 \cdot \text{ALT/AST ratio} + 0.630 \cdot \text{Diabetes mellitus (yes = 1, no = 0)} - 9.960})}{(1 + e^{0.315 \cdot \text{BMI} + 2.421 \cdot \text{ALT/AST ratio} + 0.630 \cdot \text{Diabetes mellitus (yes = 1, no = 0)} - 9.960})} * 100$

FLI, fatty liver index; NAFLD-LFS, non-alcoholic fatty liver disease liver fat score; HIS, hepatic steatosis index

3. MRI protocol

Imaging was performed on a clinical 3T MR system (MAGNETOM Skyra; Siemens Healthcare, Erlangen, Germany) using a combination of a 30-channel body and a 32-channel spine matrix coil. Subjects were examined in supine position, and all images were acquired in an expiratory breath-hold. In each subject, 3 slices were acquired for T1 mapping and 3 slices for MRE, and the locations for T1 mapping and MRE were identical. The following non-contrast enhanced sequences were performed in all subjects:

(A) Multi-echo Dixon water-fat separation was performed to evaluate the liver fat and iron content with the following parameters: TE, 1.05/2.46/3.69/4.92/6.15/7.38 ms; TR, 9.00 ms; flip angle, 4 degrees;

field-of-view (FOV), $450 \times 393 \text{ mm}^2$; matrix, 160×111 ; slice thickness, 3.5 mm; number of slices, 72; parallel imaging acceleration, 2×2 ; acquisition time, 13 s. Multi-echo Dixon sequences were performed sequentially. MRI-based proton density fat fraction (MRI-PDFF) maps and screening and multi-echo Dixon reports were provided through the scanner reconstruction (Fig. 2).

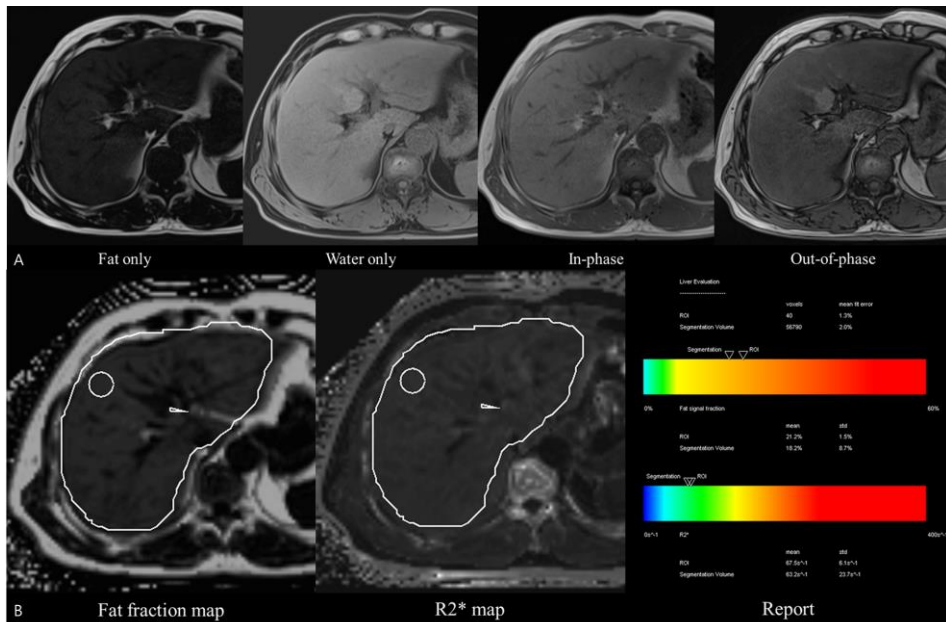


Figure 2. Multi-echo Dixon sequences and fat fraction map of a 58-year-old-male with hepatic steatosis (21.2%). (A) Axial T1-weighted two-point Dixon technique included fat and water images, and in- and out-of-phase images. (B) T1-independent T2*-corrected multi-echo Dixon technique quantifies fat/water content and R2* value in each voxel and provides a report based on the region of interest as well as whole liver segmentation.

(B) T1 mapping was performed using a prototypical Look-Locker sequence.

For each acquired slice, the sequence performed continuous fast low-angle shot (FLASH) acquisitions following an inversion pulse, providing images at multiple inversion times T1. Three slices were obtained for each patient. Sequence parameters were as follows: TR, 3.2 ms; TE, 1.32 ms; 16 TIs at 122, 347, 572, 797, 1022, 1247, 1472, 1697, 1922, 2147, 2372, 2597, 2822, 3047, 3272, and 3497 ms; flip angle, 8 degrees; FOV, $380 \times 309 \text{ mm}^2$; matrix, 192×125 ; slice thickness, 5 mm; acquisition time, 11 s. Calculation of the T1 parameter maps was integrated into the scanner reconstruction and was based on a single-compartment model, i.e., assuming that the signal evolution at a given image position is described by a single T1 relaxation time.

(C) For MRE, continuous longitudinal mechanical waves at 60 Hz were generated using an acoustic pressure driver device on the anterior chest wall. A prototype spin-echo echo-planar imaging sequence was acquired during breath-holding in three axial planes (using the same slices as in T1 mapping) with the following parameters: TR, 500 ms; TE, 39 ms; FOV, $380 \times 309 \text{ mm}^2$; matrix, 100×100 ; slice thickness, 5 mm; GRAPPA acceleration factor, 2; and acquisition time, 6 s.

4. Imaging analysis

On each slice of the obtained T1 and MRE stiffness maps, regions of interest (ROIs) were manually drawn to include only the parenchyma of the liver by two observers who had 5 years and 6 years of experience in performing MRE, respectively. The corresponding magnitude, anatomical, and wave images were simultaneously evaluated to avoid areas immediately beneath the driver, the bile ducts, blood vessels, and any other regions with incoherent wave propagation. Measurements were restricted to areas where the confidence parameter of the stiffness reconstruction was above 95%.^{26,27} Liver stiffness was measured from

the ROI drawn in this way, and the ROI was copied and pasted onto the T1 map of the same slice to obtain the T1 relaxation time. The observers averaged the T1 relaxation time and liver stiffness from the values obtained from the three manually drawn ROIs (one ROI in each slice). A custom drawing program (Singo.via, version VB30; Siemens, Erlangen, Germany) was used for the imaging analysis (Fig. 3). To assess repeatability, two measurement sessions were performed at 2-week intervals. The observers were blinded to the participants' biochemical and fat quantification data. After two measurements, 2 weeks apart, one of the two observers recorded the fat fraction and R2* derived from multi-echo Dixon acquisitions for each subject. Liver iron concentration (LIC) was calculated using the conversion formula of R2*, $LIC (\mu\text{mol}) = R2^*/3.2$.²⁸ Hepatic steatosis based on MRI-PDFF was graded according to the following criteria: 6.4% for grade 0 vs ≥ 1 , 16.3% for grade ≤ 1 vs 2, 21.7% for \leq grade 2 vs 3.²⁹⁻³¹

5. Statistical analyses

Baseline characteristics were calculated using descriptive statistics. Normality of the distribution was evaluated using the Shapiro–Wilk test. Normally distributed data were described as mean and standard deviation (SD). The correlations between T1 value and fat fraction obtained by MRI-PDFF, and between T1 value and liver stiffness obtained by MRE, were assessed using Pearson's correlation coefficient (r). The independent two-sample t -test was used to evaluate the difference in T1 relaxation time according to the presence or absence of hepatic steatosis predicted according to MRI-PDFF, FLI, NAFLD-LFS, and HSI. One-way analysis of variance (ANOVA) was used for intergroup comparisons of T1 value according to the steatosis grade based on MRI-PDFF. In addition, the independent two-sample t -test was used to evaluate the differences in T1 values according to the presence or absence of hepatic

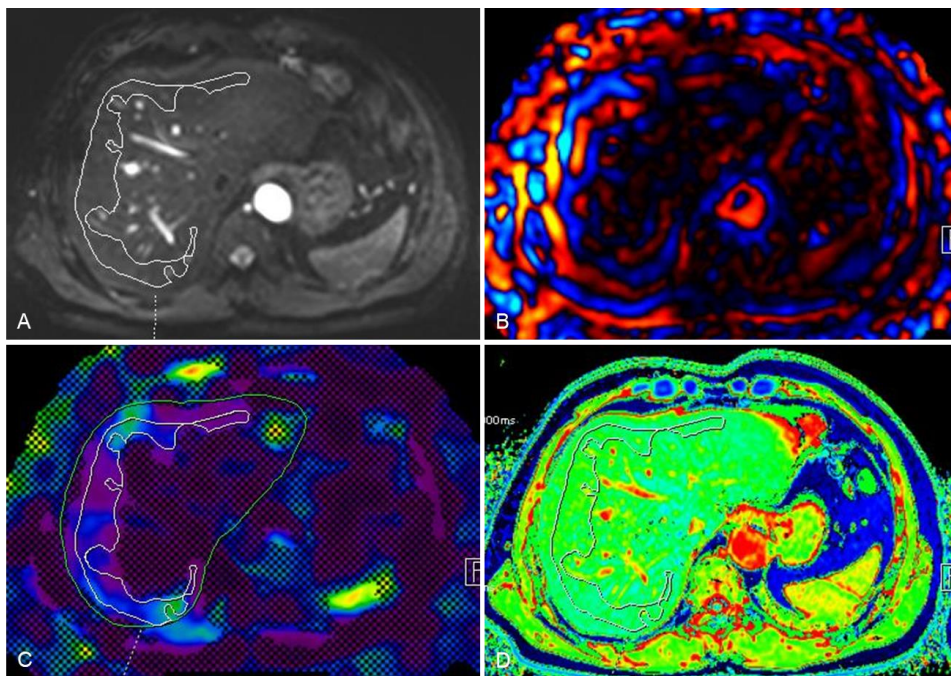


Figure 3. Representative measurement of liver stiffness and T1 relaxation time using magnetic resonance elastography and T1 mapping, respectively. A. A manual region of interest (ROI) drawn on the magnitude image of a 45-year-old-female with hepatic steatosis (15%). B. Imaging showing wave propagation. A manual ROI copied on to the stiffness map with 95% confidence map (C) and T1 map (D).

fibrosis predicted by MRE. Univariate and multiple linear regression analyses were also performed to determine whether other variables influenced the T1 value and liver stiffness obtained by MRE. The multiple linear relationships were estimated with stepwise selection, and the best multiple linear regression model was selected. In these analyses, laboratory data were used as binary

variables (normal versus abnormal) because the laboratory data had no clinical significance when the values were normal.

The reproducibility between two readers and repeatability of liver stiffness measurement using MRE and T1 mapping were evaluated by determining intraclass correlation coefficients (ICCs). An ICC value of >0.81 was considered to indicate almost perfect agreement, while values of 0.61–0.80, 0.41–0.60, and 0.21–0.40 represented substantial, moderate, and fair agreement, respectively. Statistical significance was set at $P < 0.05$.

Statistical analysis was performed using a commercially available software (SAS, version 9.4, SAS Institute, Cary, NC, USA, and R software, version 3.6.3, R Development Core Team, Vienna, Austria).

III. RESULTS

1. Subjects

Hepatic steatosis was assessed based on an MRI-PDFF threshold of 6.4%;^{29,30} 133 of 340 subjects had hepatic steatosis. The mean MRI-PDFF was $11.7 \pm 4.9\%$ in the group with hepatic steatosis and $3.3 \pm 1.4\%$ in the groups without hepatic steatosis. The number of subjects by steatosis grade was 207 for grade 0, 115 for grade 1, 13 for grade 2, and 5 for grade 3. Hepatic fibrosis was assessed based on MRE threshold of 2.9 kPa;^{26,27,32} 22 of 340 subjects had hepatic fibrosis. Subject characteristics are summarized in Table 2.

2. Correlation between fat fraction from MRI-PDFF and liver stiffness of MR elastography and T1 value

T1 relaxation time showed a positive correlation with the fat fraction obtained from MRI-PDFF ($r=0.615$, $P < 0.001$) and with the liver stiffness obtained from MRE ($r=0.370$, $P < 0.001$) (Fig. 4).

3. T1 value according to hepatic steatosis and liver stiffness

When assessing hepatic steatosis according to MRI-PDFF, T1 values were significantly increased for hepatic steatosis. The mean T1 value was 817.58 ± 52.77 ms (range, 679.05–1015.45 ms) for subjects without hepatic steatosis and 899.79 ± 89.71 ms (range, 666.28–1258.99 ms) for subjects with hepatic steatosis ($P < 0.001$). Even when the presence of hepatic steatosis was predicted using FLI, NAFLD-LFS, and HSI, T1 values were significantly increased in subjects with hepatic steatosis (Table 3). When comparing hepatic steatosis grades based on MRI-PDFF, the mean T1 values were significantly different in

Table 2. Demographic and laboratory characteristics of study subjects.

Parameter	All subjects (n=340)
Gender	
Male	122 (35.9%)
Female	218 (64.1%)
Age (y)	66.3±7.3
Body mass index (kg/m ²)	25.44±3.27
Waist circumference (cm)	87.69±50.27
Diabetes (%)	75 (22%)
AST (IU/L)	24.86±16.96
ALT (IU/L)	21.77±25.19
Serum albumin level (g/dL)	4.64±0.23
Gamma-glutamyltransferase (U/L)	28.89±29.16
Platelet count (x10 ⁹ /L)	236.15±57.20
Cholesterol level (mg/dL)	176.97±35.32
Triglyceride (mg/dL)	159.71±102.20
Proton density fat fraction (%)	6.5±5.2
Liver stiffness at MRE (kPa)	2.15±0.50
T1 relaxation time (ms)	849.74±80.25
R2* (s ⁻¹ Hz)	48.85±9.99
Calculated liver iron concentration (μmol)	15.27±3.12

AST, aspartate aminotransferase; ALT, alanine aminotransferase; MRE, magnetic resonance elastography

Data are means ± standard deviation.

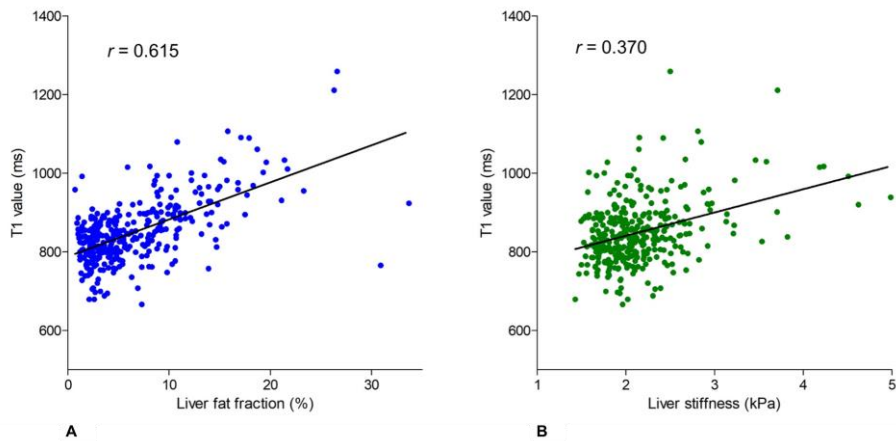


Figure 4. Pearson's correlation coefficient. A. Correlation between T1 value by T1 mapping and liver fat fraction. There is significant positive correlation (Pearson's $r = 0.615$). B. Correlation between T1 value by T1 mapping and liver stiffness by MRE. There is weak positive correlation (Pearson's $r = 0.370$).

Table 3. T1 relaxation time of study subjects classified according to hepatic steatosis.

	With hepatic steatosis		Without hepatic steatosis		<i>P</i> value
	n	T1 relaxation time (ms)	n	T1 relaxation time (ms)	
MRI-PDFF	133	899.79±89.71	207	817.58±52.77	<0.001
FLI	71	910.73±101.23	269	836.64±65.00	<0.001
NAFLD-LFS	141	890.66±84.91	199	820.74±62.38	<0.001
HSI	249	862.03±82.40	91	816.09±63.12	<0.001

MRI-PDFF, MRI-based proton density fat fraction; FLI, fatty liver index; NAFLD-LFS, non-alcoholic fatty liver disease liver fat score; HSI, hepatic steatosis index

Data are means ± standard deviation.

all grades, and the T1 value tended to increase as the grade increased ($P < 0.001$, P for trend < 0.001) (Fig. 5).

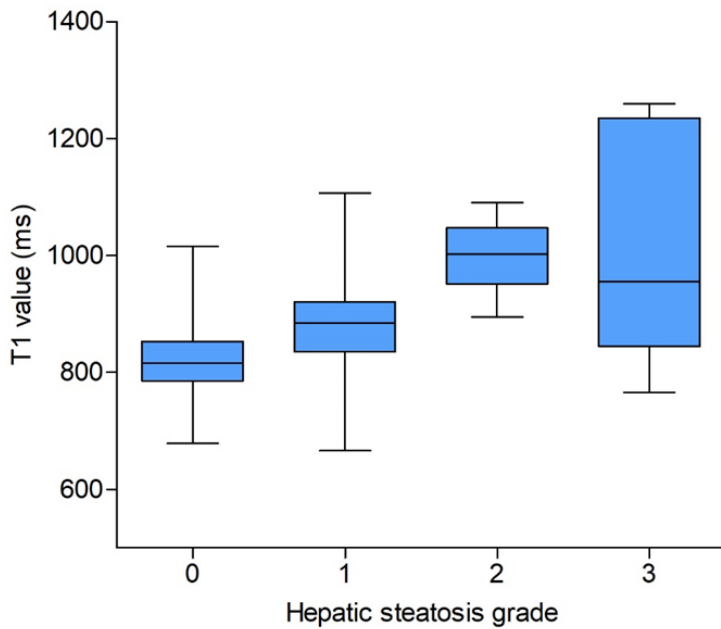
When assessing liver stiffness according to MRE, T1 values were significantly increased in hepatic fibrosis. The mean T1 value was 843.62 ± 75.98 ms (range, 666.28–1258.99 ms) for subjects with liver stiffness less than 2.9 kPa, and 938.08 ± 89.84 ms (range, 814.96–1211.01 ms) for subjects with liver stiffness greater than 2.9 kPa ($P < 0.001$).

4. Univariate and multiple linear regression analyses for variables affecting the T1 value and liver stiffness of MRE

In the univariate analysis, MRI-PDFF, calculated LIC, liver stiffness, and AST were significantly associated with T1 value. Three statistical multiple linear regression models were constructed, and the best multiple linear regression models for T1 value were those containing MRI-PDFF, calculated LIC, liver stiffness, and AST with an R square of 0.546 (Table 4). In the univariate analysis, T1 value, AST, GGT, and BMI were significantly associated with liver stiffness obtained by MRE, whereas MRI-PDFF and calculated LIC were not significantly associated (Table 5).

5. Reproducibility and repeatability of the MR elastography and T1 mapping

ICCs for the reproducibility and repeatability of the liver stiffness values obtained using MRE and liver T1 value using T1 mapping are summarized in Table 6. The ICC values indicated a near-perfect agreement.



Hepatic steatosis grade	n	T1 relaxation time (ms)	<i>P</i> value	<i>P</i> for trend
0	207	817.58±25.78	<0.001	<0.001
1	115	883.20±73.19		
2	13	999.15±60.71		
3	5	1022.87±207.22		

Figure 5. Box and whisker plot of the T1 relaxation time according to the hepatic steatosis grade. The mean T1 relaxation times were significantly different between each steatosis grade, and tended to increase as the grade increased.

Table 4. Results of univariate and multiple linear regression analysis of T1 value

Parameter	Univariate analysis			Multivariate analysis		
	Coefficient (β)	SE*	<i>P</i> value	Coefficient (β)	SE*	<i>P</i> value
Body mass index (kg/m ²)	2.073	1.067	0.053			
Waist circumference (cm)	0.043	0.059	0.465			
AST (IU/L)	29.675	11.482	0.010	28.982	11.112	0.010
Serum albumin level (g/dL)	-11.734	54.332	0.829			
Gamma-glutamyltransferase (U/L)	3.925	9.184	0.669			
Platelet count (x10 ⁹ /L)	-9.021	17.611	0.609			
Cholesterol level (mg/dL)	-12.942	6.937	0.063			
Triglyceride (mg/dL)	13.331	7.238	0.066			
Proton density fat fraction (%)	10.084	0.682	<0.001	10.514	0.624	<0.001
Liver stiffness at MRE (kPa)	22.278	7.078	0.002	29.309	6.414	<0.001
Calculated LIC (μ mol)	-8.959	1.031	<0.001	-9.153	1.018	<0.001

*Standard error of the estimated coefficient.

ALT was not included due to collinearity with AST.

SE, standard error. AST, aspartate aminotransferase; MRE, magnetic resonance elastography; LIC, liver iron concentration.

Table 5. Results of univariate and multiple linear regression analysis of liver stiffness at MRE

Parameter	Univariate analysis			Multivariate analysis		
	Coefficient (β)	SE*	<i>P</i> value	Coefficient (β)	SE*	<i>P</i> value
Gender	-0.020	0.052	0.701			
Age (y)	0.006	0.003	0.062			
Body mass index (kg/m ²)	0.043	0.008	<0.001	0.038	0.007	<0.001
Waist circumference (cm)	0.000	0.000	0.684			
AST (IU/L)	0.324	0.088	<0.001	0.331	0.085	<0.001
Serum albumin level (g/dL)	0.003	0.421	0.994			
Gamma-glutamyltransferase (U/L)	0.335	0.066	<0.001	0.339	0.063	<0.001
Platelet count (x10 ⁹ /L)	0.084	0.136	0.536			
Cholesterol level (mg/dL)	-0.038	0.053	0.473			
Triglyceride (mg/dL)	0.084	0.056	0.138			
Proton density fat fraction (%)	-0.012	0.007	0.085			
T1 relaxation time (ms)	0.001	0.000	0.001	0.001	0.000	<0.001
Calculated LIC (μ mol)	-0.003	0.009	0.733			

*Standard error of the estimated coefficient.

ALT was not included due to collinearity with AST.

SE, standard error. AST, aspartate aminotransferase; MRE, magnetic resonance elastography; LIC, liver iron concentration.

Table 6. Reproducibility and repeatability of measurements obtained by MRE and T1 mapping.

	MRE		T1 relaxation time	
	ICC (95% CI)	<i>P</i> value	ICC (95% CI)	<i>P</i> value
Interobserver reproducibility	0.955 (0.948-0.962)	<0.001	0.995 (0.994-0.996)	<0.001
Repeatability				
Reader 1	0.983 (0.980-0.987)	<0.001	0.996 (0.995-0.997)	<0.001
Reader 2	0.936 (0.921-0.949)	<0.001	0.990 (0.988-0.992)	<0.001

MRE, magnetic resonance elastography; ICC, intraclass correlation coefficient; CI, confidence interval

IV. DISCUSSION

This study demonstrates that T1 value by T1 mapping is significantly correlated with liver fat content, and hepatic steatosis is significantly associated with an increased T1 value. In addition to the liver fat fraction, the T1 value is also influenced by liver iron content, inflammation, and liver stiffness.

Various studies have been conducted on non-invasive diagnostic methods for early detection and grading of hepatic fibrosis in CLD including NAFLD. MRE is the most accurate non-invasive method for the detection and staging of hepatic fibrosis, and it is not significantly influenced by age, sex, degree of inflammation, steatosis, or etiology of CLD.^{13,33} In our study, liver stiffness measured by MRE was not affected by age, sex, and MRI-PDFF, nor by calculated LIC. However, measurement failure may occur due to increased iron deposition, obesity, and ascites, and additional hardware and software are required.^{13,26,34} Diffusion-weighted imaging can be performed on most MR scanners and has the advantage of not requiring additional devices, but it is not suitable for early hepatic fibrosis detection.^{35,36} Texture analysis is a useful tool for excluding fibrosis in patients with liver disease, but it has the disadvantage of being influenced by the technical quality of the source image and requiring additional texture analysis software.^{37,38} The hepatobiliary phase T1 relaxation time measurement on gadoxetic acid-enhanced MRI is reportedly useful for diagnosing hepatic fibrosis. However, hepatobiliary agent injection is required, and hepatobiliary phase imaging takes at least 20 minutes, which is disadvantageous because of its long examination time.^{38,39} Various serologic markers are also used to predict hepatic fibrosis, but most have high accuracy for advanced hepatic fibrosis and low diagnostic accuracy for early fibrosis.⁴⁰⁻⁴²

In contrast, T1 mapping is a simple sequence that can be used without contrast agents or additional devices. Recent studies reported the potential of

native T1 mapping for the diagnosis of hepatic fibrosis and as a predictor of clinical outcomes in patients with CLD.^{15,43,44}

Previous studies have reported increased T1 relaxation time owing to hepatic parenchymal fibrosis,^{14,16,17} but no other factors, such as fat, iron, or inflammation, that could affect T1 values have been evaluated. Another study reported that fat tissue had a short T1 value, and that T1 in regions of visceral fat measured using T1 mapping is short.⁴⁵ Another study conducted using 1.5T MRI for factors affecting the T1 value reported that fibrosis, iron concentration, and inflammation significantly affected the T1 relaxation time, but fat did not.²⁰ However, another study using 3T MRI reported that the T1 value was affected by hepatic steatosis,¹⁹ and in our study, the T1 value was also affected by liver fat content; in both studies, the T1 relaxation time was longer in the presence of fatty liver. There were differences in the number of subjects with steatosis and the T1 value itself according to the methods for evaluating hepatic steatosis, but these results were the same regardless of the evaluation method.

The difference between our study and the previous studies on the effects of liver fat content on the T1 value is thought to be due to the technique used for T1 mapping, the difference in MRI field strength, and the difference in the fat fraction of the tissues. T1 measurement by inversion and saturation recovery methods currently used for T1 mapping assumes a single species (e.g., water or fat) and a mono-exponential curve fit is performed to derive a single T1 value. As in hepatic steatosis, water and fat coexist in the tissue, and a mixture of water and fat has a bi-exponential recovery curve in proportion to their relative fractions. In this condition, the curve fitting with mono-exponential recovery produces a single T1 value and results in an error called the partial volume effect.^{19,46} At 3T, the chemical shift of fat is larger than that at 1.5T, and the fat is generally out-of-phase with water. In out-of-phase mixture of water and fat, the signal is subtracted by the fat component, resulting in slow T1 recovery and longer T1 relaxation time. According to previous studies, the T1 value increases

in an approximately linear fashion with the fat fraction when the fat fraction is less than approximately 30%.^{19,46} In our study, the subjects showed less than 30% fat fraction except for two subjects, and the T1 value increased significantly as the hepatic steatosis grade according to MRI-PDFF increased.

This issue is significant in that hepatic fibrosis may be overestimated when assessed in patients with NAFLD using the current T1 mapping sequence in 3T MRI. This is because the current T1 mapping uses a mono-exponential curve fitting of water and fat, so it is considered necessary to develop a new T1 mapping sequence that separates water and fat to solve this problem. Although related studies such as magnetic resonance fingerprinting with dictionary-based fat and water separation have been recently reported, no commercialized T1 mapping sequence is available yet.^{47, 48}

In a recent study, the correlation coefficient between MRE and T1 mapping was reported as 0.34–0.48, which is similar to that in our study ($r=0.37$).⁴⁹ However, unlike our study, the effects of fat and inflammation were not evaluated. In the multiple linear regression analysis of our study, we found that PDFF, calculated LIC, liver stiffness, and abnormal serum AST level influenced T1 value. In other words, the T1 value can be influenced not only by fat, but also by several factors such as liver stiffness, iron concentration, and inflammation as shown in previous studies.

Hepatic fibrosis has been known as a useful indicator for predicting mortality in patients with NAFLD,⁵⁰ and MRE is the most accurate non-invasive method for the evaluation of hepatic fibrosis. However, the pathogenesis of NAFLD is complex and should be evaluated by reflecting not only fibrosis, but also steatosis and inflammation. Therefore, the enrollment criteria for NASH clinical trials typically require patients to not only have evidence of Kleiner-Brunt fibrosis stage (F) ≥ 2 , but also a NAFLD Activity Score (NAS) ≥ 4 . Recently, reflecting this trend, several composite scores such as the FibroScan-AST (FAST) score,⁵¹ cT1-AST-fasting glucose (cTAG) score,⁵²

and a blood-based biomarker panel (NIS4)⁵³ have been reported. In particular, cTAG is a biomarker identified by a combination of iron-corrected T1 mapping, AST, and fasting glucose, and it has been reported as a good predictor of $F \geq 2$ and $NAS \geq 4$ (area under the curve, 0.90). However, in this study, the effect of fat on the T1 value was not evaluated. According to the results of our study, since T1 value is affected by fat, iron, liver stiffness, and inflammation, we deemed it necessary to obtain a T1 value that corrected for all these factors. Therefore, in order to develop more accurate composite biomarkers using T1 mapping, further research based on histopathological results is needed.

A major limitation of this study was the absence of histopathological results. However, liver biopsies in the cohort group were not considered feasible for ethical reasons. Among the non-invasive diagnostic methods of hepatic steatosis and hepatic fibrosis, MRI-PDFF and MRE have been reported to have very high diagnostic accuracy.^{30-32,34,54,55} Therefore, in this study, steatosis and liver stiffness were evaluated by performing MRI-PDFF and MRE instead of liver biopsy. In addition, the presence of hepatic steatosis was also evaluated using hepatic steatosis indices, and the difference in T1 values according to the analyzed hepatic steatosis showed a similar trend as the results of evaluation through MRI-PDFF. In this study, as reported in other studies, liver stiffness measured by MRE was not affected by MRI-PDFF and calculated LIC. However, it was affected by AST, GGT, and BMI. In nonadvanced fibrosis ($F \leq 2$), inflammation may increase liver stiffness and act as a confounding factor in the diagnosis of hepatic fibrosis.⁵⁶ Since most of the subjects in our study had no or nonadvanced fibrosis, it is thought that liver stiffness measured by MRE was affected by AST and GGT. Furthermore, it is known that liver stiffness measured by MRE is not affected by BMI in advanced fibrosis;⁵⁷ however, the effect of BMI in the absence of fibrosis is not clearly established. In our study, liver stiffness measured by MRE was influenced by BMI. Unfortunately, it is difficult to explain the reason for this within the scope of

this study. Our study had many subjects without fibrosis, and further studies based on histopathology are needed to determine how BMI affects MRE in these cases. Another limitation was that 22 subjects had hepatic fibrosis by MRE even though subjects with CLD other than hepatic steatosis were excluded from the study. This is thought to be because the exclusion criteria were not strict enough to screen out unknown medical history in all subjects because CLD was investigated through clinical history.

V. CONCLUSION

The T1 value obtained by current T1 mapping of 3T MRI was affected by the liver fat component and several other factors such as liver stiffness, iron concentration, and inflammation. Therefore, T1 adjustment considering these confounders may improve the diagnostic ability of T1 value for assessing patients with NAFLD.

REFERENCES

1. Loomba R, Sanyal AJ. The global NAFLD epidemic. *Nat Rev Gastroenterol Hepatol*. 2013;10:686-90.
2. Younossi ZM. Non-alcoholic fatty liver disease - A global public health perspective. *J Hepatol*. 2019;70:531-44.
3. Rinella ME. Nonalcoholic fatty liver disease: a systematic review. *JAMA*. 2015;313:2263-73.
4. Fazel Y, Koenig AB, Sayiner M, Goodman ZD, Younossi ZM. Epidemiology and natural history of non-alcoholic fatty liver disease. *Metabolism*. 2016;65:1017-25.
5. Dulai PS, Singh S, Patel J, Soni M, Prokop LJ, Younossi Z, et al. Increased risk of mortality by fibrosis stage in nonalcoholic fatty liver disease: Systematic review and meta-analysis. *Hepatology*. 2017;65:1557-65.
6. Colloredo G, Guido M, Sonzogni A, Leandro G. Impact of liver biopsy size on histological evaluation of chronic viral hepatitis: the smaller the sample, the milder the disease. *J Hepatol*. 2003;39:239-44.
7. McGill DB, Rakela J, Zinsmeister AR, Ott BJ. A 21-year experience with major hemorrhage after percutaneous liver biopsy. *Gastroenterology*. 1990;99:1396-400.
8. Dowman JK, Tomlinson JW, Newsome PN. Systematic review: the diagnosis and staging of non-alcoholic fatty liver disease and non-alcoholic steatohepatitis. *Aliment Pharmacol Ther*. 2011;33:525-40.
9. Talwalkar JA. Elastography for detecting hepatic fibrosis: options and considerations. *Gastroenterology*. 2008;135:299-302.
10. Talwalkar JA, Yin M, Fidler JL, Sanderson SO, Kamath PS, Ehman RL. Magnetic resonance imaging of hepatic fibrosis: emerging clinical applications. *Hepatology*. 2008;47:332-42.
11. Asbach P, Klatt D, Hamhaber U, Braun J, Somasundaram R, Hamm B, et al.

- Assessment of liver viscoelasticity using multifrequency MR elastography. *Magn Reson Med*. 2008;60:373-9.
12. Wagner M, Corcuera-Solano I, Lo G, Esses S, Liao J, Besa C, et al. Technical Failure of MR Elastography Examinations of the Liver: Experience from a Large Single-Center Study. *Radiology*. 2017;284:401-12.
13. Mathew RP, Venkatesh SK. Imaging of hepatic fibrosis. *Curr Gastroenterol Rep*. 2018;20:45.
14. Thomsen C, Christoffersen P, Henriksen O, Juhl E. Prolonged T1 in patients with liver cirrhosis: an in vivo MRI study. *Magn Reson Imaging*. 1990;8:599-604.
15. Banerjee R, Pavlides M, Tunncliffe EM, Piechnik SK, Sarania N, Philips R, et al. Multiparametric magnetic resonance for the non-invasive diagnosis of liver disease. *J Hepatol*. 2014;60:69-77.
16. Cassinotto C, Feldis M, Vergniol J, Mouries A, Cochet H, Lapuyade B, et al. MR relaxometry in chronic liver diseases: Comparison of T1 mapping, T2 mapping, and diffusion-weighted imaging for assessing cirrhosis diagnosis and severity. *Eur J Radiol*. 2015;84:1459-65.
17. Heye T, Yang SR, Bock M, Brost S, Weigand K, Longerich T, et al. MR relaxometry of the liver: significant elevation of T1 relaxation time in patients with liver cirrhosis. *Eur Radiol*. 2012;22:1224-32.
18. Hamdy A, Kitagawa K, Ishida M, Sakuma H. Native Myocardial T1 Mapping, Are We There Yet? *Int Heart J*. 2016;57:400-7.
19. Mozes FE, Tunncliffe EM, Pavlides M, Robson MD. Influence of fat on liver T1 measurements using modified Look-Locker inversion recovery (MOLLI) methods at 3T. *J Magn Reson Imaging*. 2016;44:105-11.
20. Hoad CL, Palaniyappan N, Kaye P, Chernova Y, James MW, Costigan C, et al. A study of T₁ relaxation time as a measure of liver fibrosis and the influence of confounding histological factors. *NMR Biomed*. 2015;28:706-14.

21. Huh JH, Ahn SV, Koh SB, Choi E, Kim JY, Sung KC, et al. A Prospective Study of Fatty Liver Index and Incident Hypertension: The KoGES-ARIRANG Study. *PLoS One*. 2015;10: e0143560.
22. Kim JY, Ahn SV, Yoon JH, Koh SB, Yoon J, Yoo BS, et al. Prospective study of serum adiponectin and incident metabolic syndrome: the ARIRANG study. *Diabetes Care*. 2013;36:1547-53.
23. Bedogni G, Bellentani S, Miglioli L, Masutti F, Passalacqua M, Castiglione A, et al. The Fatty Liver Index: a simple and accurate predictor of hepatic steatosis in the general population. *BMC Gastroenterol*. 2006;6:33.
24. Kotronen A, Peltonen M, Hakkarainen A, Sevastianova K, Bergholm R, Johansson LM, et al. Prediction of non-alcoholic fatty liver disease and liver fat using metabolic and genetic factors. *Gastroenterology*. 2009;137:865-72.
25. Lee JH, Kim D, Kim HJ, Lee CH, Yang JI, Kim W, et al. Hepatic steatosis index: a simple screening tool reflecting nonalcoholic fatty liver disease. *Dig Liver Dis*. 2010;42:503-8.
26. Venkatesh SK, Ehman RL. Magnetic resonance elastography of liver. *Magn Reson Imaging Clin N Am*. 2014;22:433-46.
27. Guglielmo FF, Venkatesh SK, Mitchell DG. Liver MR Elastography Technique and Image Interpretation: Pearls and Pitfalls. *Radiographics*. 2019;39:1983-2002.
28. Henninger B, Alustiza J, Garbowski M, Gandon Y. Practical guide to quantification of hepatic iron with MRI. *Eur Radiol*. 2020;30:383-93.
29. Tang A, Tan J, Sun M, Hamilton G, Bydder M, Wolfson T, et al. Nonalcoholic fatty liver disease: MR imaging of liver proton density fat fraction to assess hepatic steatosis. *Radiology*. 2013;267:422-31.
30. Tang A, Desai A, Hamilton G, Wolfson T, Gamst A, Lam J, et al. Accuracy of MR imaging-estimated proton density fat fraction for classification of dichotomized histologic steatosis grades in nonalcoholic fatty liver disease. *Radiology*. 2015;274:416-25.

31. Middleton MS, Heba ER, Hooker CA, Bashir MR, Fowler KJ, Sandrasegaran K, et al.; NASH Clinical Research Network. Agreement Between Magnetic Resonance Imaging Proton Density Fat Fraction Measurements and Pathologist-Assigned Steatosis Grades of Liver Biopsies From Adults With Nonalcoholic Steatohepatitis. *Gastroenterology*. 2017;153:753-61.
32. Hoodeshenas S, Yin M, Venkatesh SK. Magnetic Resonance Elastography of Liver: Current Update. *Top Magn Reson Imaging*. 2018;27:319-33.
33. Singh S, Venkatesh SK, Wang Z, Miller FH, Motosugi U, Low RN, et al. Diagnostic performance of magnetic resonance elastography in staging liver fibrosis: a systematic review and meta-analysis of individual participant data. *Clin Gastroenterol Hepatol*. 2015;13:440-51.
34. Chen J, Talwalkar JA, Yin M, Glaser KJ, Sanderson SO, Ehman RL. Early detection of nonalcoholic steatohepatitis in patients with nonalcoholic fatty liver disease by using MR elastography. *Radiology*. 2011;259:749-56.
35. Wang QB, Zhu H, Liu HL, Zhang B. Performance of magnetic resonance elastography and diffusion-weighted imaging for the staging of hepatic fibrosis: A meta-analysis. *Hepatology*. 2012;56:239-47.
36. Papalavrentios L, Sinakos E, Chourmouzi D, Hytiroglou P, Drevelegas K, Constantinides M, et al. Value of 3 Tesla diffusion-weighted magnetic resonance imaging for assessing liver fibrosis. *Ann Gastroenterol*. 2015;28:118-23.
37. House MJ, Bangma SJ, Thomas M, Gan EK, Ayonrinde OT, Adams LA, et al. Texture-based classification of liver fibrosis using MRI. *J Magn Reson Imaging*. 2015;41:322-8.
38. Petitclerc L, Sebastiani G, Gilbert G, Cloutier G, Tang A. Liver fibrosis: Review of current imaging and MRI quantification techniques. *J Magn Reson Imaging*. 2017;45:1276-95.
39. Ding Y, Rao SX, Meng T, Chen C, Li R, Zeng MS. Usefulness of T1

mapping on Gd-EOB-DTPA-enhanced MR imaging in assessment of non-alcoholic fatty liver disease. *Eur Radiol.* 2014;24:959-66.

40. Harrison SA, Oliver D, Arnold HL, Gogia S, Neuschwander-Tetri BA. Development and validation of a simple NAFLD clinical scoring system for identifying patients without advanced disease. *Gut.* 2008;57:1441-7.

41. McPherson S, Stewart SF, Henderson E, Burt AD, Day CP. Simple non-invasive fibrosis scoring systems can reliably exclude advanced fibrosis in patients with non-alcoholic fatty liver disease. *Gut.* 2010;59:1265-9.

42. Adams LA, George J, Bugianesi E, Rossi E, De Boer WB, van der Poorten D, et al. Complex non-invasive fibrosis models are more accurate than simple models in non-alcoholic fatty liver disease. *J Gastroenterol Hepatol.* 2011;26:1536-43.

43. Ramachandran P, Serai SD, Veldtman GR, Lang SM, Mazur W, Trout AT, et al. Assessment of liver T1 mapping in fontan patients and its correlation with magnetic resonance elastography-derived liver stiffness. *Abdom Radiol (NY).* 2019;44:2403-8.

44. Li J, Liu H, Zhang C, Yang S, Wang Y, Chen W, et al. Native T1 mapping compared to ultrasound elastography for staging and monitoring liver fibrosis: an animal study of repeatability, reproducibility, and accuracy. *Eur Radiol.* 2020;30:337-45.

45. de Bazelaire CM, Duhamel GD, Rofsky NM, Alsop DC. MR imaging relaxation times of abdominal and pelvic tissues measured in vivo at 3.0 T: preliminary results. *Radiology* 2004;230:652-9.

46. Kellman P, Bandettini WP, Mancini C, Hammer-Hansen S, Hansen MS, Arai AE. Characterization of myocardial T1-mapping bias caused by intramyocardial fat in inversion recovery and saturation recovery techniques. *J Cardiovasc Magn Reson.* 2015;17:33.

47. Cencini M, Biagi L, Kaggie JD, Schulte RF, Tosetti M, Buonincontri G. Magnetic resonance fingerprinting with dictionary-based fat and water

- separation (DBFW MRF): A multi-component approach. *Magn Reson Med.* 2019;81:3032-3045.
48. Koolstra K, Webb AG, Veeger TTJ, Kan HE, Koken P, Börnert P. Water-fat separation in spiral magnetic resonance fingerprinting for high temporal resolution tissue relaxation time quantification in muscle. *Magn Reson Med.* 2020;84:646-662.
49. Hoffman DH, Ayoola A, Nickel D, Han F, Chandarana H, Shanbhogue KP. T1 mapping, T2 mapping and MR elastography of the liver for detection and staging of liver fibrosis. *Abdom Radiol.* 2020;45:692-700.
50. Ekstedt M, Hagström H, Nasr P, Fredrikson M, Stål P, Kechagias S, et al. Fibrosis stage is the strongest predictor for disease-specific mortality in NAFLD after up to 33 years of follow-up. *Hepatology.* 2015;61:1547-54.
51. Newsome PN, Sasso M, Deeks JJ, Paredes A, Boursier J, Chan WK, et al. FibroScan-AST (FAST) score for the non-invasive identification of patients with non-alcoholic steatohepatitis with significant activity and fibrosis: a prospective derivation and global validation study. *Lancet Gastroenterol Hepatol.* 2020;5:362-373.
52. Dennis A, Mouchti S, Kelly M, Fallowfield JA, Hirschfield G, Pavlides M, et al. A composite biomarker using multiparametric magnetic resonance imaging and blood analytes accurately identifies patients with non-alcoholic steatohepatitis and significant fibrosis. *Sci Rep.* 2020;10:15308.
53. Harrison SA, Ratziu V, Boursier J, Francque S, Bedossa P, Majd Z, et al. A blood-based biomarker panel (NIS4) for non-invasive diagnosis of non-alcoholic steatohepatitis and liver fibrosis: a prospective derivation and global validation study. *Lancet Gastroenterol Hepatol.* 2020;11:970-985.
54. Kim D, Kim WR, Talwalkar JA, Kim HJ, Ehman RL. Advanced fibrosis in nonalcoholic fatty liver disease: noninvasive assessment with MR elastography. *Radiology.* 2013;268:411-9.
55. Park CC, Nguyen P, Hernandez C, Bettencourt R, Ramirez K, Fortney L, et

al. Magnetic Resonance Elastography vs Transient Elastography in Detection of Fibrosis and Noninvasive Measurement of Steatosis in Patients With Biopsy-Proven Nonalcoholic Fatty Liver Disease. *Gastroenterology*. 2017;152:598-607.

56. Shi Y, Guo Q, Xia F, Dzyubak B, Glaser KJ, Li Q, et al. MR Elastography for the Assessment of Hepatic Fibrosis in Patients with Chronic Hepatitis B Infection: Does Histologic Necroinflammation Influence the Measurement of Hepatic Stiffness? *Radiology*. 2014;273: 88–98.

57. Singh S, Venkatesh SK, Wang Z, Miller FH, Motosugi U, Low RN, et al. Diagnostic performance of magnetic resonance elastography in staging liver fibrosis: a systematic review and meta-analysis of individual participant data. *Clin Gastroenterol Hepatol*. 2015;13:440-451.e6.

ABSTRACT(IN KOREAN)

비알콜성지방간질환 환자를 대상으로 한 3T 자기공명영상의 T1 mapping 기법에서 간 지방증이 T1 이완시간 평가에 미치는 영향

<지도교수 유 정 식>

연세대학교 대학원 의학과

안 지 현

목적: 이 연구는 3T 자기공명영상에서 native T1 mapping의 T1 이완시간이 지방 성분에 의해 영향을 받는지 조사하고자 하였다.

재료 및 방법 : 이 전향적 연구에는 인구 기반 코호트로부터 2018년 5월 8일부터 2019년 8월 8일까지 340명의 참가자가 참여하였고, 참가자들로부터 다음과 같은 데이터를 획득하였다:(1) 자기공명탄성영상을 통한 간의 강성도; (2) T1 mapping을 통한 T1 이완시간; (3) 자기공명영상 기반 양성자 밀도 지방분율(MRI-PDF); (4) 체질량지수, 허리둘레, 당뇨 과거력, 아스파르테이트아미노전달효소, 알라닌아미노전달효소, 감마글루타밀전달효소, 트리글리세라이드를 활용한 간 지방증 지표들. Pearson의 상관계수 분석을 통해 간의 강성도 및 지방분율과 T1 이완시간 간의 상관성을 평가하였다. 독립표본 t-검정을 이용하여 지방간 여부에 따른 T1 이완시간의 차이를 평가하였고, MRI-PDF 수치를 이용한 지방간 등급에 따른 T1 이완시간의 차이는 일원배치분산분석을 통해 평가하였다. 추가적으로, T1 이완시간에 영향을 미치는 변수들을 알아보기 위해 다중 선형회귀분석을 시행하였다.

결과 : T1 이완시간은 MRI-PDF와 양의 상관관계를 보였고($r=0.615$, P

< 0.001), 자기공명탄성영상을 통해 획득한 간의 강성도와 양의 상관관계를 보였다 ($r=0.370$, $P < 0.001$). 지방간의 평가 방법의 종류에 관계없이 지방간이 있는 경우에 T1 이완시간이 유의하게 증가하였다 ($P < 0.001$). MRI-PDFF를 기반으로 하여 지방간 등급을 나누어 비교하였을 때, 평균 T1 이완시간은 등급별로 차이가 있었으며 등급이 증가할수록 T1 이완시간이 증가하는 경향을 보였다 ($P < 0.001$, P for trend < 0.001). 다중 선형회귀분석에서 MRI-PDFF, 간의 철 성분, 간의 강성도, 그리고 아스파르테이트아미노전달효소가 T1 이완시간에 영향을 미치는 것으로 나타났다.

결론 : 3T 자기공명영상장치에서 현재의 T1 mapping을 통해 획득한 T1 이완시간은 간의 지방 성분 및 간의 강성도, 간의 철 성분, 염증과 같은 요인들의 영향을 받는다.

핵심되는 말 : T1 mapping, T1 이완시간, 지방간, 비알콜성지방간, 간 강성도, 간섬유화

PUBLICATION LIST

1. Ahn JH, Yu JS, Park KS, Kang SH, Huh JH, Chang JS, et al. Effect of hepatic steatosis on native T1 mapping of 3T magnetic resonance imaging in the assessment of T1 values for patients with non-alcoholic fatty liver disease. *Magn Reson Imaging* 2021;80:1-8. doi: 10.1016/j.mri.2021.03.015.